Master's Thesis of Engineering

Experimental and Thermodynamical Studies on the Development of Smart Structural Binder

스마트 구조 결합재 개발을 위한 실험적 및 열역학적 연구

February 2023

Graduate School of Civil and Environmental Engineering
Seoul National University
Smart City Engineering Major
Jihoon Lee

Experimental and Thermodynamical Studies on the Development of Smart Structural Binder

Jae-Yeol Cho

Submitting a master's thesis of
Civil and Environmental Engineering

February 2023

Graduate School of Civil and Environmental
Engineering
Seoul National University
Smart City Engineering Major

Jihoon Lee

Confirming the master's thesis written by
Jihoon Lee
February 2023

Chair	_____	(Seal)
Vice Chair	_____	(Seal)
Examiner	_____	(Seal)

Abstract

A sustainable and smart structural binder has to be developed for achieving the global target of carbon neutrality since there is no alternative of Ordinary Portland Cement which emits a large amount of CO_2 during its manufacturing process. In US and Europe, there has been steady efforts to improve the sustainability of cementitious materials which results in the commercialization of smart structural binder with 35% inclusion of limestone powder. However, Korean standard still allows only 5% inclusion of limestone powder.

This study aims to increase the limestone powder content for enhancing the sustainability of structural materials. The hydration reaction of type 1 ordinary Portland cement (OPC) with increasing limestone powder replacement was investigated using thermodynamic modelling. X-ray powder diffraction (XRD) and Rietveld refinement were used to analyze the hydration. A combination of isothermal calorimetry, compressive strength, differential scanning (DSC)-thermogravimetric (TG), and thermodynamic modelling were used to understand the complex chemical variations. The result of thermodynamic modelling indicates that the limestone powder cannot be participated in the hydration reaction even with a 15% inclusion of limestone regardless of water to cement ration. On the other hand, with the increase of C_3A content in the clinker, limestone partly reacted with existing hydration products. The hydration reaction produced monocarboaluminate (Mc) which substantially contributed to the strength enhancement. In addition, curing

temperature also plays an important role. In actual experiments with mechanochemically activated PLC, the advanced specific surface area and aluminate reaction in PLC improve the mechanical property more than OPC although the limestone powder substituted the 20 % of clinker, generating a more quantity of Mc. Therefore, it is concluded that aluminate content and appropriate curing temperature can be necessary to improve the performance and advanced limestone reaction. The study conducted herein can provide a pathway to develop a sustainable and smart structural binders without compromising material performance.

TABLE OF CONTENTS

1. INTORDUTION

1.1. Background and Motivation

Cement, one of the most widely used materials in the world, is now blamed for carbon dioxide emissions. C_3S, C_3A, C_2S, and C_4AF, the main constituent minerals of cement clinker, are basically produced through the calcination of limestone. For this reason, carbon dioxide emissions in the cement manufacturing process are reported to account for about 11% of the total carbon dioxide emissions in the industry, and specifically, about 800 kg of carbon dioxide is emitted when producing 1 ton of cement clinker [1]. Therefore, changes in the cement industry are inevitable in the current trend of curbing carbon dioxide emissions worldwide, and numerous related studies are also being actively conducted.

. Portland limestone cement (PLC) has been used to reduce CO2 emissions by reducing the clinker production. The investigation for using limestone powder as SCMs has been studied since the fly ash and ground granulated blast-furnace slag (GGBFS) supply chains are threatened [2, 3]. The pressure for 'carbon neutral' promotes the usage of PLC. EN 197-1 designates two classes of PLC as CEM II/A-L and CEM II/B-L in which the maximum contents of limestone are 20 % and 35 %, respectively. Many specifications enable Portland

cement to contain limestone up to 5 % since the small limestone replacement does not influence its mechanical properties and durability compared with limestone-free cement [4]. However, there has not yet a separate PLC standard in Korea, and the use of limestone in cement is usually allowed less than 5% of Portland cement based on KSL 5201.

the limestone powder can enhance the hydration reaction by filler effect and reaction with aluminate, which results in the production of hemicarboaluminate (Hc) and monocarboaluminate (Mc) with the small amount of limestone [5]. Alumina plays important role in the mechanical performance of PLC. When the SCMs such as slag and metakaolin are used, the mechanical properties of limestone blended cement increased in spite of the 10 % of limestone substitution. Unfortunately, more than 10 % replacement of limestone diminished the performance of PLC [6, 7]. Eventually, an increase in the limestone content of PLC to reduce carbon dioxide emissions causes a decrease in concrete quality, and research should be conducted to solve this problem.

1.2. Objective and scope

As a basic study for developing Korean limestone cement, this research aims to explore the change in the hydration reaction and mechanical performance of cement with increasing limestone content through thermodynamic modeling using Gibbs free energy. In addition, thermodynamic modelling is carried out based on the specific surface area, mineral composition change, and curing temperature of clinker including limestone.

Based on the results of thermodynamic modelling, PLC was mechanochemically activated and assorted experiments were carried out, including isothermal conduction calorimetry, X-ray diffraction (XRD), and thermogravimetry. Blaine air permeability method and particle laser analyzer were used to confirm the physical change affected by mechanochemical activation (MA). In the experiment part of this study, the aim of this research is to analyze the change of hydration reaction, phase assemblage, and mechanical performance of PLC by different limestone powder substitution to develop an understanding of the mechanochemical activation effect. Crude pulverization clinker, gypsum, and limestone powder were blended to explore the effect on the hydration and mechanical properties of PLC.

2. MATERIALS AND METHODS

2.1. Thermodynamic Modelling

2.1.1. Materials for thermodynamic modelling

In this study, thermodynamic modeling was conducted using type 1 OPC. The results of X−ray diffraction measurement of Portland cement are shown in Figure 1. The XRD data was measured by D2 phaser X−ray diffractometer (Bruker Co. Ltd., Germany) equipped with Cu−Kα radiation ($\lambda = 1.5418\,\text{Å}$) in the range of 2θ between 5° and 60°. The collected XRD data were analyzed using HighScore Plus software 4.8 (PANalytical, Netherlands) with the inorganic crystal structure database (ICSD) [8] and the crystallography open database (COD) [9].
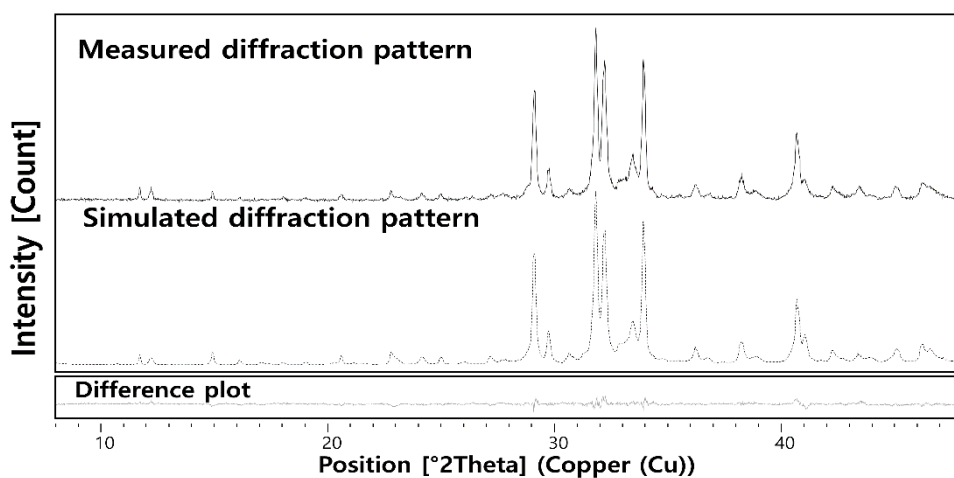
Figure. 1. Measured and simulated X−ray diffraction pattern of raw OPC.

As a result of X—ray diffraction analysis, the main constituent materials of cement were clinker, with C3S, C2S, C3A, and C4AF accounting for 92.4% of the total weight, with 55.1%, 22.2%, 4.8%, and 10.3%, respectively. The results of X—ray diffraction analysis are shown in Table. 1, and thermodynamic modeling was performed based on the results of the mineral composition.

Table. 1. QXRD result (%) of raw OPC.

Chemical composition [g/100g]	Weight(%)
Alite (C_3S)	55.1
Belite (C_2S)	22.2
Aluminate (C_3A)	4.8
Ferrite (C_4AF)	10.3
Gypsum	2.2
Periclase (MgO)	2.4
Lime (C)	1.4
Arcanite (K_2SO_4)	1.6
Thenardite (Na_2SO_4)	0.6

2.1.2. Database of thermodynamic modelling

The input variables and indexes for performing thermodynamic modeling are shown in Table 2. Clinker was defined as a mixture from which gypsum was removed from the quantitative analysis of X-ray diffraction of type 1 OPC mentioned above. Therefore, REF means 95% clinker and 5% gypsum, and LS5, LS10, and LS15 are samples substituted with 5% limestone, 10% and 15% for 5% gypsum, respectively. For the prediction of hydration reactions according to curing day, the hydration degree model of OPC developed by Parrot and Killoh was used. The phase assemblage of the PLC system was calculated, using using the Gibbs free energy minimization software, GEM-Selektor v.3.9.5 [10, 11]. The thermodynamic database, cemdata 18 [12], for solid, solid-solution, and aqueous phases encountered in hydration products was applied.

Table. 2. Mixture proportion for GEMS simulation

Index	Clinker (%)	Limestone (%)	Gypsum (%)	W/B
REF	95	0		
LS_5	90	5		
LS_10	85	10	5	0.5
LS_15	80	15		

The extended Debye－Hückel equation [13] was implemented to calculate the activity coefficients for aqueous species in the cement system, given as Eq (1).

$$log_{10}\gamma_i = \frac{-A_\gamma z_i^2 \sqrt{I}}{1+\dot{a}B_\gamma\sqrt{I}} + b_\gamma I + log_{10}\frac{X_{jw}}{X_w}$$
(1)

Where γ_i and z_i refer to the activity coefficient and charge of the ith aqueous species, respectively; A_γ is a temperature coefficient; B_γ is a pressure coefficient; I means the molar ionic strength of the pore solution; X_{jw} is the molar quantity of water; X_w is the total molar amount of the aqueous phase; $\dot{a}$ and b_γ are a common ion size parameter, and a short－range interaction parameter, each. $\dot{a}$ was set to 3.67 Å and b_γ was determined to 0.123 kg/mol to simulate KOH dominated electrolyte aqueous solution [5, 14]. In this simulation, temperature and pressure were respectively set to 20 ℃ and 1 bar.

2.2. Experiments

2.2.1. Materials

Crude pulverization clinker refers to a material before gypsum is added and ground in the cement production. This clinker was calcined at 850 ℃ for 3 hours to remove calcite and filtered out through a No. 30 (600 μm) sieve. Then, gypsum and limestone powder were blended into the calcined crude pulverization clinker and were milled using McCrone micronizing mill (McCrone Scientific Ltd, London, UK) for 15 minutes. The substitution contents of limestone (0 %, 10 %, 20 %) to clinker and the status of mechanochemical activation were variables in this study. The chemical and mineralogical compositions of the materials, as given in Table 3 and Table 4, were ascertained by X-ray fluorescence (XRF) and XRD/Rietveld analysis. The indexes and mixture conditions of all samples are given in Table 5. The concentration of an activator was 0.1 % of the binder.

Table. 3. Chemical composition of the materials

Chemical composition [g/100 g]	CCPC	Limestone	Gypsum
CaO	64.80	45.32	34.9
SiO_2	21.90	11.30	1.52
Al_2O_3	5.33	1.59	0.62
Fe_2O_3	3.02	0.52	0.24
MgO	2.83	1.99	0.57
K_2O	0.83	0.56	0.06
SO_3	0.53	0.62	43.78
TiO_2	0.28	0.07	< 0.01
P_2O_5	0.21	0.06	< 0.01
Loss of ignition	< 0.01	37.80	18.20

Table 4. Phase composition of materials

Phase composition [g/100 g]	CCPC	Limestone
Alite (C_3S)	50.3	-
Belite (C_2S)	30.4	-
Aluminate (C_3A)	3.2	-
Ferrite (C_4AF)	11.2	-
Periclase	2.9	-
Lime	1.5	-
Arcanite	0.5	-
Calcite	-	86.3
Quartz	0.2	10.0
Dolomite	-	2.9
Zeolite	-	0.4

Table 5. The mixture condition of samples

Mixture	CCPC (%)	Gypsum (%)	Limestone (%)	Activator(%)
LS0_0	95	5	-	-
LS0_0.1	95	5	-	0.1
LS10_0	85	5	10	-
LS10_0.1	85	5	10	0.1
LS20_0	75	5	20	-
LS20_0.1	75	5	20	0.1

2.2.2. Sample preparation

All pastes were prepared with distilled water to cement ratio (W/C) of 0.5 and deionized water was used to make pastes. The indexes and mixture conditions of all samples are given in Table 3. Isothermal conduction calorimetry, XRD, and differential scanning (DSC)−thermogravimetric (TG) experiments were carried with with cement pastes. The compressive strength test was carried out using both cement paste (W/C = 0.5). XRD and DSC−TG were examined with 1 day, 3 days, 7 days, and 28 days hydrated samples in the 20 ℃ and 60 % of relative humidity curing condition. The powders were immersed in isopropyl alcohol and ethyl ether to stop the hydration

reaction by removing free water from the cement paste. Then, the ethyl ether was evaporated by drying up to 40 ℃ for 40 minutes [15–17].

2.2.3. Isothermal calorimetry

The heat of hydration of PLC was measured by a TAM Air system (TA Istruments, USA) at 20 ± 0.02 ℃. After the steady baseline was maintained for 2 hours at a constant external room temperature, 20 ℃, 4 g of deionized water was added to 8 g of each mixture. Subsequently, the cement pastes were mixed for 2 minutes before pouring it into glass ampoules. The glass ampoules were sealed by aluminum lids and placed into the calorimeter. The heat which is released by the hydration reaction was evaluated for 3 days.

2.2.4. X–ray diffraction

The XRD data was measured by D2 phaser X–ray diffractometer (Bruker Co. Ltd., Germany) equipped with Cu–Kα radiation (λ = 1.5418 Å) in the range of 2θ between 5° and 60°. The collected XRD data were analyzed using HighScore Plus software 4.8 (PANalytical, Netherlands) with the inorganic crystal structure database (ICSD) [8] and the crystallography open database (COD) [9].

2.2.5. Thermogravimetry analysis

The change of weight of paste by raising temperature was gauged by SDT Q600 (TA Instrumdnt, Ltd., USA) heating from 20 ℃ to 1000 ℃. The heating rate of all samples was 10 ℃/min under the condition that the flow rate of N_2 gas was 100 mL/min.

3. RESULTS AND DISCUSSION

3.1. Results of Thermodynamic modelling

3.1.1. Predicted phase assemblages of Portland limestone cement

Since the volume of the hydrate product is directly related to the pores inside the cement paste, the volume of the hydrate product has a positive correlation in which the compressive strength increases as the volume of the hydrate product increases. The prediction model of each sample using the hydration degree model of Parrot and Killoh is illustrated in figure. 2－5. Regardless of the content of limestone, it can be observed that limestone remains constant from the beginning of the hydration reaction. After the start of hydration, the reaction began rapidly from the first day of curing, and the decomposition of etrringite did not occur due to the relatively high gypsum content, 5%. Also, the amount of C_3A contained in the binder decreased, hence increasing the value of SO_3/Al_2O_3 and the value of CO_2/Al_2O_3. In this case, limestone inside the binder does not participate in the hydration reaction [18]. Since the increase in the limestone content reduces the proportion of clinker in the binder, the voids inside the cement paste increase and the compressive strength decreases.
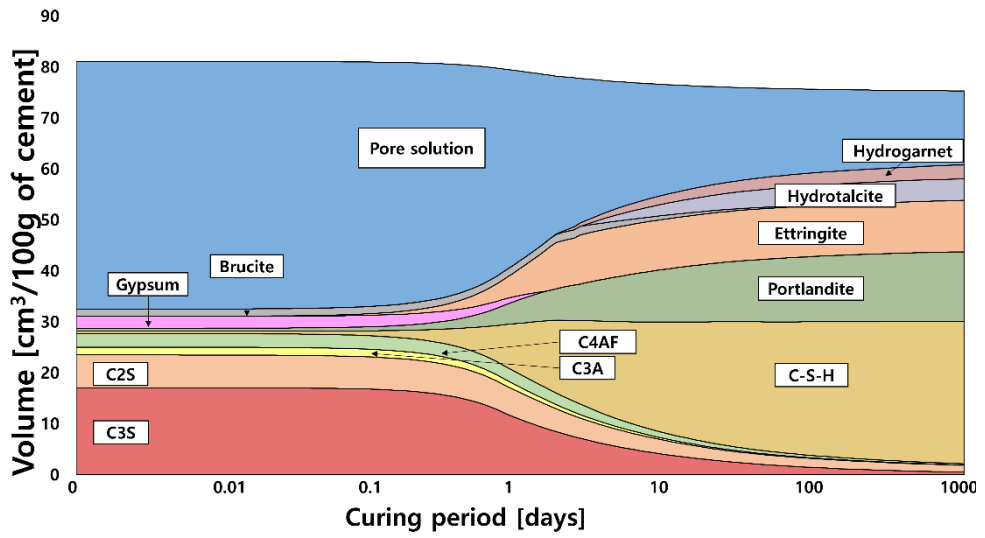
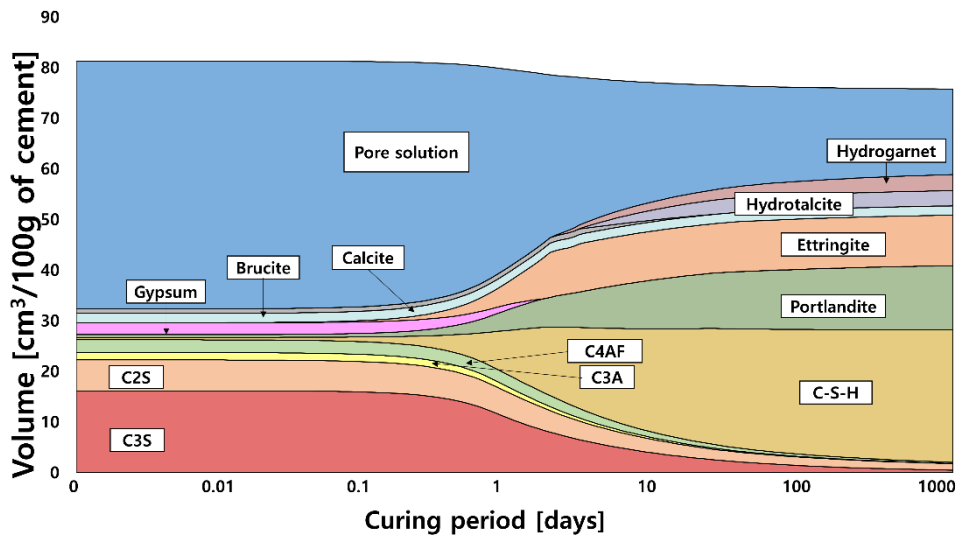Figure. 2. Predicted phase assemblages of REF samples

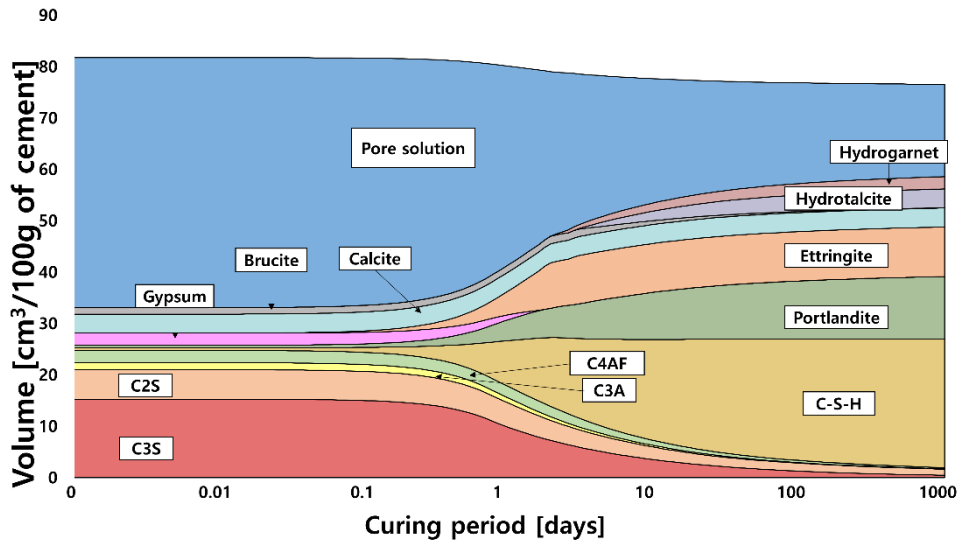Figure. 3. Predicted phase assemblages of LS5 samples

1 5

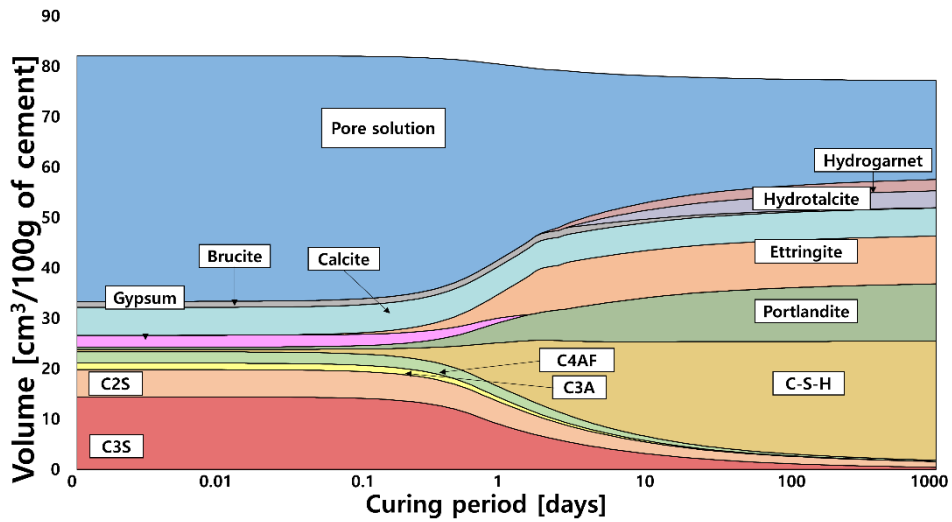Figure. 4. Predicted phase assemblages of LS10 samples

Figure. 5. Predicted phase assemblages of LS15 samples
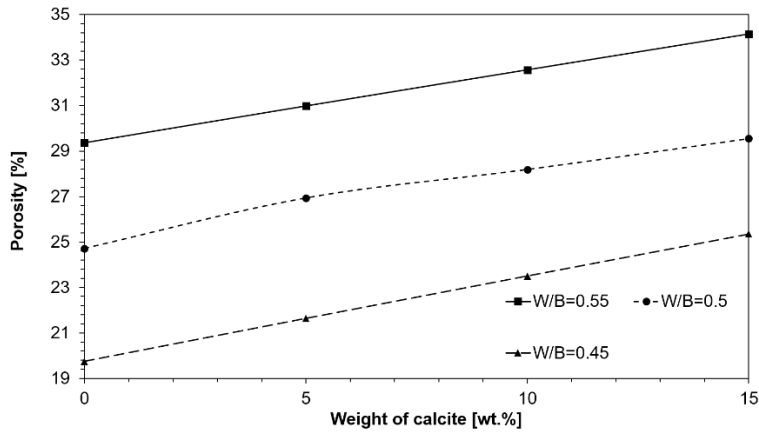
3.1.2. Effect of water to cement ratio

Figure. 6. Predicted porosity of cement pastes with different W/B
(0.45, 0.50, 0.55) as a function of included limestone content

Figure 6 shows the change in porosity on the 28th day of curing
when the limestone content was increased according to the water-
binder ratio (W/B). As W/B increases, the porosity inside the cement
paste increases by nature. When the content of limestone is 0%, the
porosity tends to increase to 19.74%, 24.71%, and 29.37%, as the
W/B increases to 0.45, 0.5, and 0.55. For W/B=0.45, the porosity
increases to 21.64%, 23.51%, and 25.35%, by increasing the
limestone content from 0% to 5%, 10%, and 15%. When W/B=0.5, it
increases to 26.93%, 28.19%, and 29.55%, and tends to increase to
30.99%, 32.57%, and 34.14%, respectively, for W/B=0.55. These
results show that limestone does not chemically participate in the
hydration reaction even if the water-binder ratio (W/B) is raised. In
addition, increasing W/B in limestone cement with low clinker content

1 7

may cause relatively greater performance degradation. Since it does not participate in this chemical reaction, increasing the limestone content increases the porosity regardless of W/B, thereby lowering the compressive strength. In addition, the porosity and the compressive strength of concrete are not just linear relationships, but exponential functions, so the higher the W/B, the greater the loss of compressive strength [19].

3.1.3. Effect of aluminate content

Figure 7 and 8 shows the hydration reaction prediction model when the mass ratio of C_3A contained in the binder is increased by 2 and 3 times the content of gypsum, respectively. As the content of C_3A increases, it can be seen that the AFm phase is produced from day 3 of the hydration reaction. As the content of C_3A increases, the amount of limestone participating in the reaction increases, and thus the amount of Mc produced increases. As a result, compared to the conventional hydration reaction, the volume of the hydration product increases and the strength lost due to the increase in the limestone content may be recovered. In addition, this Mc production reaction starts later than potlandite and C-S-H production reactions and proceeds even after curing, which helps to enhance post-strength,

thereby increasing the strength of limestone cement paste in the long term [5, 18, 20].
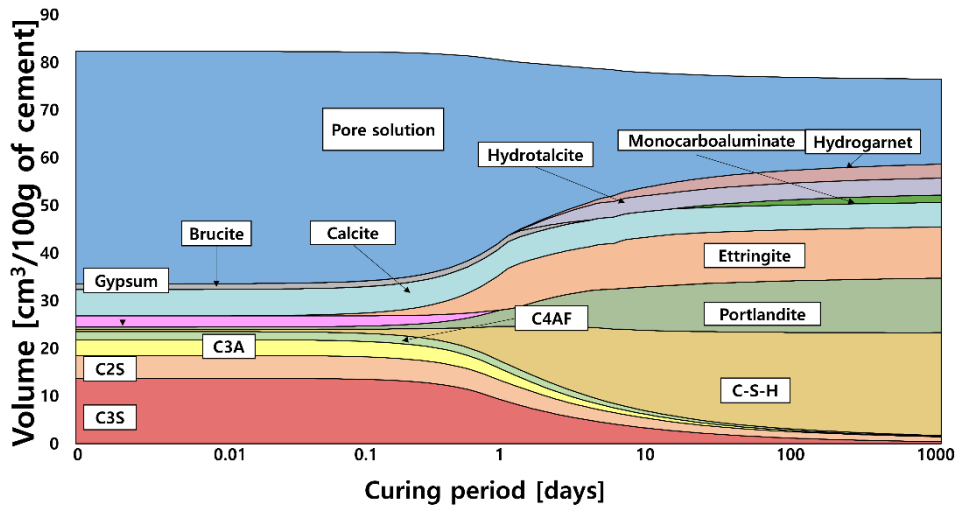
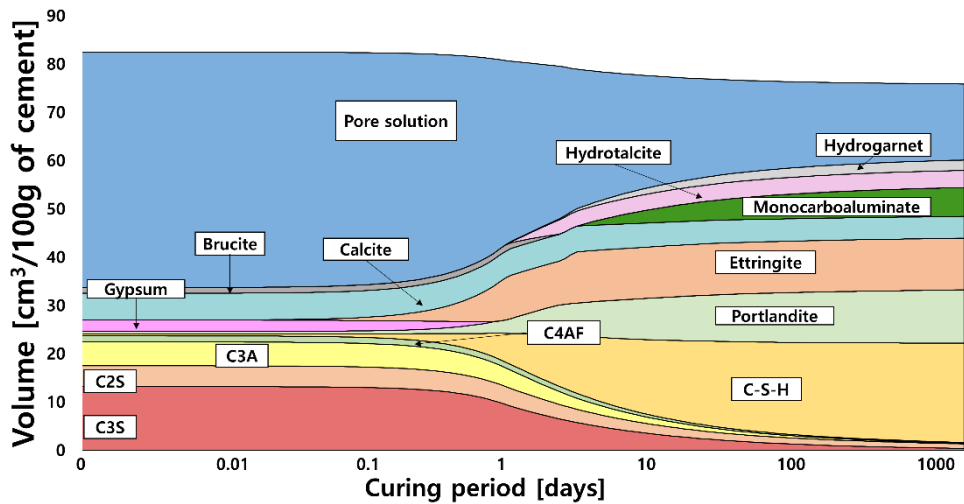Figure 7. Predicted phase assemblages of C$_3$A 10 % LS15

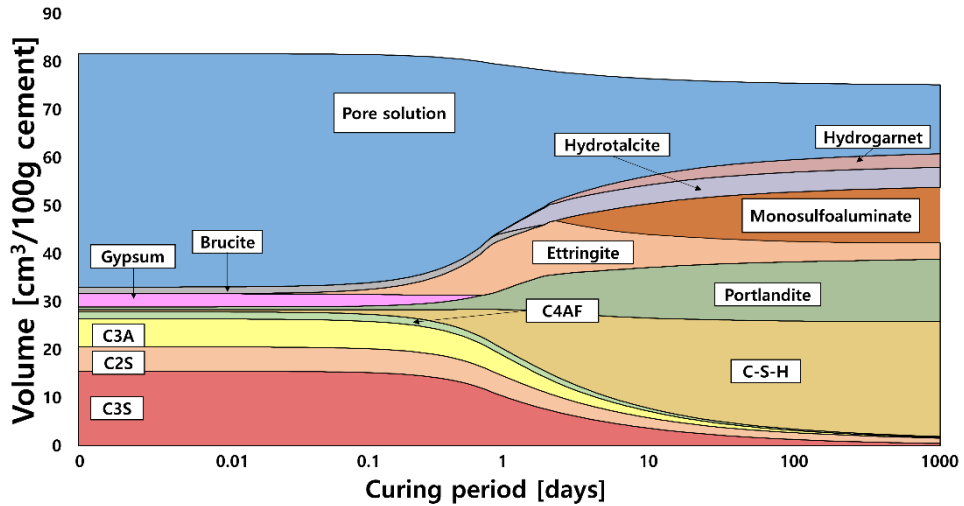Figure 8. Predicted phase assemblages of C$_3$A 15 % LS15

Figure 9. Predicted phase assemblages of C₃A REF

Figure 9 illustrates the hydration reaction prediction when the content of C3A is 15% and the limestone powder is not present. Decomposition of ettringite begins on day 3 of the hydration reaction, producing monosulfate (Ms). At this time, surfate ions present outside the concrete react with Ms to produce ettringite, which expands in volume, resulting in cracks in the concrete, reducing its mechanical performance [21]. When the content of C3A in limestone cement is increased, pores are reduced due to the stabilization of ettringite due to the generation of Mc, and resistance to penetration of sulfate into concrete is increased, thereby improving durability.
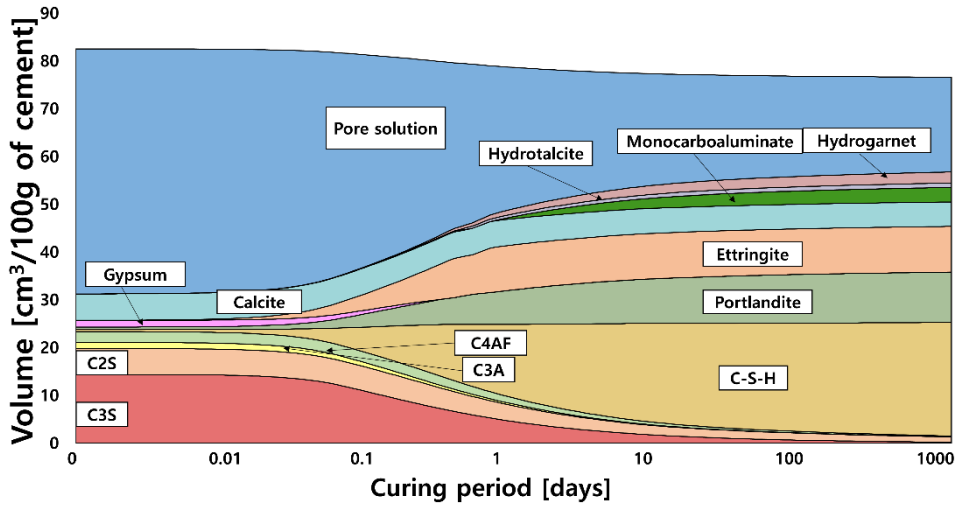
3.1.4. Effect of temperature

Figure 10. Predicted phase assemblages of LS15 during curing at 50 ˚C

Another way to engage limestone in hydration reactions is to change the curing temperature. Ettringite, one of the main hydration products of Portland cement, is unstable at temperatures above 50℃ and decomposes into Ms [12]. In this case, when the curing temperature is changed to room temperature, ettringite is generated again. When such delay of ettringite formation occurs, cracks are generated inside concrete due to volume expansion, which negatively affects compressive strength. In particular, it is a factor that greatly degrades the mechanical performance of concrete along with the drying shrinkage phenomenon due to high temperature curing [16].

Figure10 shows the hydration reaction prediction model when limestone cement containing 15% limestone is cured at 50°C. shown in 7. As the ettringite is decomposed, Mc is formed by reacting with limestone. In addition, cracks caused by dry shrinkage due to the reaction of limestone can be controlled, which acts positively on high-temperature curing concrete. However, when curing at high temperatures above 50℃, Mc is not produced and Ms is produced [22]. In other words, limestone does not participate in the hydration reaction, but rather negative effects such as delayed ettringite formation act on concrete, negatively affecting compressive strength and durability. Therefore, the limestone can be involved in the hydration reaction only when an appropriate curing temperature is set.

3.2. Results of Experiments
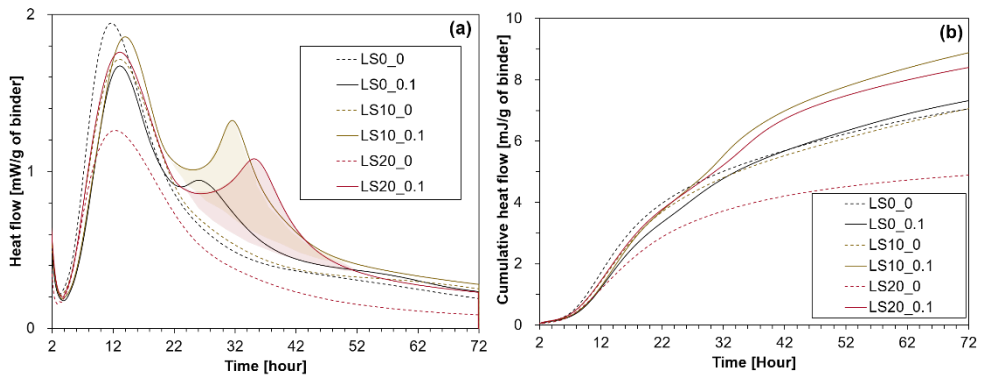
3.2.1. Hydration kinetic

Figure 11. Heat flow development (a) of samples versus times
between 0 hour and 72 hour and (b) cumulative heat.

Fig. 11 (a) represents the heat flow induced by the hydration of cement pastes. The presence of a secondary hydration peak, the production of AFm phases, proved that MA promoted the dissolution of aluminate clinker, C3A and C4AF [23]. The second peak of LS0_0.1 indicates the production of Ms since the limestone is absent. Instead, Mc was precipitated in LS10_0.1 and LS20_0.1 samples, precluding the decomposition of AFt phases from ettringite to Ms [5, 18, 24]. The peak of secondary hydration cannot be observed in the samples without MA since the molar ratio of SO3 from gypsum and Al2O3 from aluminate is 3.66 on 3 days hydration. Namely, the ratio of SO3/Al2O3 reacted in 3 days was too high to generate the secondary hydration [12, 18]. In other words, the presence of a

second peak is attributed to the fast dissolution of ferrite and aluminate [25, 26]. The reason why the appearance time of the second peak was delayed as the content of limestone in PLC increased is owing to higher the relative quantity of gypsum in PLC as the gypsum content was unchanged in all samples. Therefore, the depletion of sulfate ions in the pore solution was postponed.

Fig. 11 (b) reveals the cumulative heat flow. In the limestone-free system (LS0 samples). All samples with MA discharged more heat than those with the same replacement of limestone powder without MA until 3 days. Although the quantity of clinker was reduced in LS10 and LS20 samples, the cumulative heat from hydration was bigger than the LS0 sample when the MA was applied due to the heat emitted from calcite participation to hydration. In addition, The mechanochemically activated limestone powder accelerated the hydration of clinker by providing a nucleation site to cement [5, 27]. In the early age of hydration, the heat from the hydration of LS0_0.1 was lower than LS0_0.

3.2.2. Thermogravimetry analysis
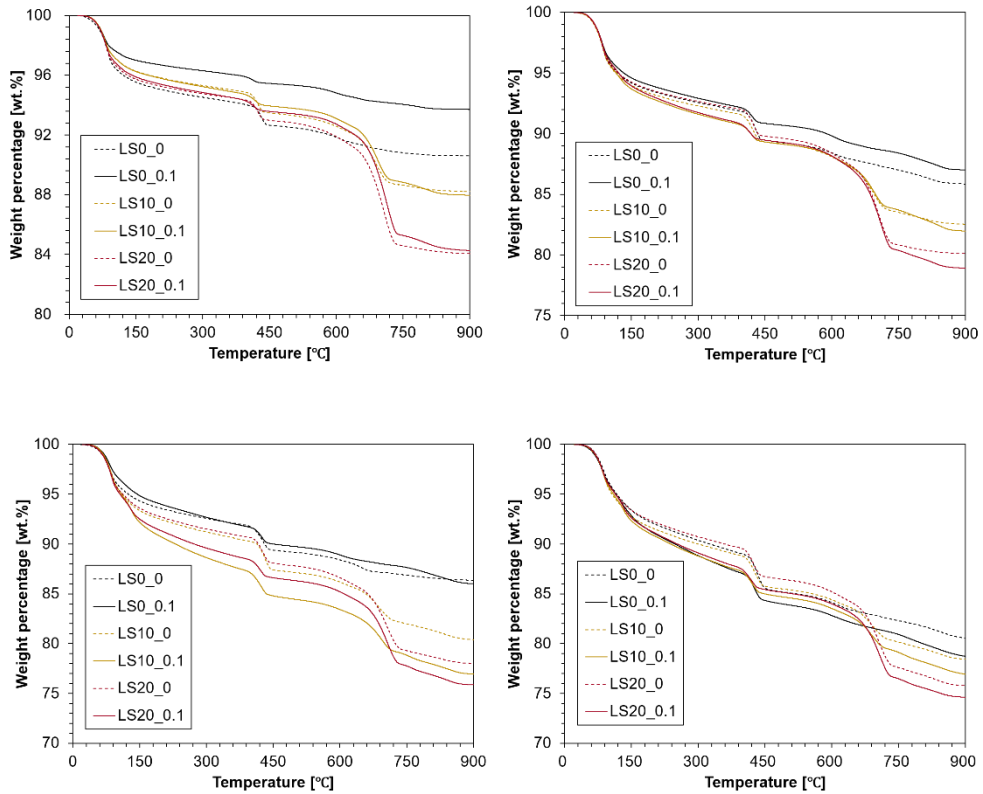
Figure 12. TG data of 1, 3, 7, and 28 days hydrated cement with and without MA

Fig. 12 illustrates the TG data that allows chemically bounded water and the quantity of hydration products such as C-S-H, ettringite, AFm phases, and portlandite to be visually recognizable. On the first day after hydration, all the samples with MA showed a lower degree of hydration than the hydrated samples without MA, especially between 300 ℃-400 ℃, which means the dehydration temperature of portlandite. The reason for the lack of compressive

strength on the first day is that the hydration reaction did not proceed in MA samples. The adsorption of activator like TEA on hydrating C_3S makes a thick layer that impedes the hydration reaction of C_3S by blocking the contact between water and clinker [29]. On the contrary, the later weight loss of the MA samples, e.g., 28 days, became greater. The complexation effect of activators was valid this effect leads to the advanced dissolution of clinker and results in higher weight loss at a later age [25, 26]. Albeit the chemically bounded water was bigger when MA was employed, the portlandite amounts were smaller regardless of the involvement of limestone. The weight loss of limestone－free samples was higher when the MA was not used until 3 days and almost same on 7 days, and then the weight loss was reversed on the 28 days. Especially, the weight loss after 100 ℃ was larger and this observation means that the amount of C－S－H, AFm phases, and Fe－siliceous hydrogarnet was produced more[30], [23]. On the hydration of 28 days, LS0_0.1 sample showed the most degree of hydration within all samples due to the amount of clinker and the effect of mechanochemical activation.
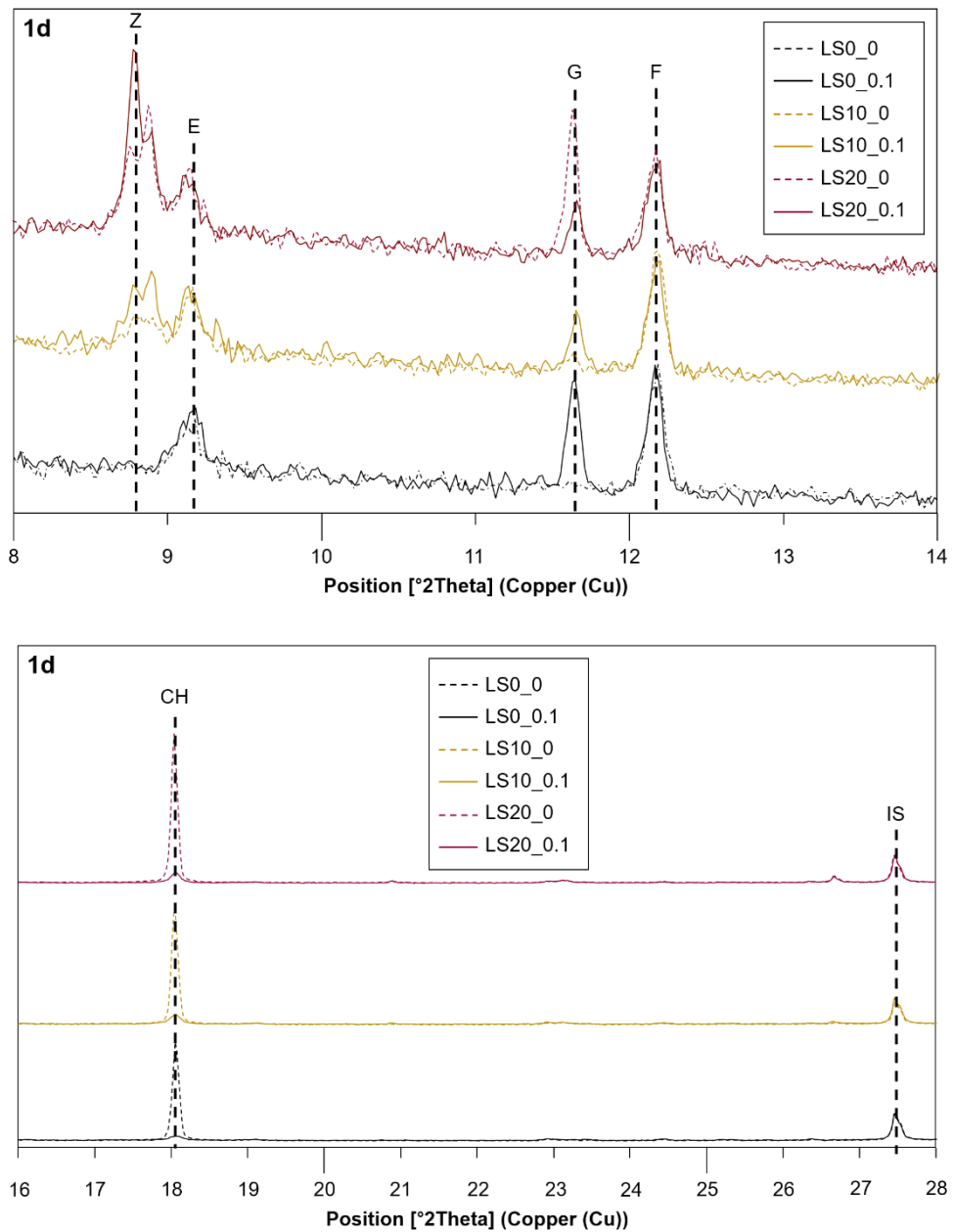
3.2.3. X-ray diffraction

Figure 13. XRD patterns of 1 day hydrated PLC paste samples (Z: zeolite, E: Ettringite, G: Gypsum, F: Ferrite, CH: portlandite, $C\bar{C}$: calcite, IS: internal standard material).

The XRD patterns of hydrated pastes after the first day are displayed in Fig. 13. TiO2 is the internal standard material that was enabled to compare the relative intensity of target materials and calculate the content of amorphous, which can not be detected by XRD. Ettringite was precipitated in all samples regardless of the usage of MA and the presence of limestone. However, the gypsum in MA pastes was not fully dissolved on 1 day, which means that alkanolamine does not only interfere with the dissolution of C_3S but also interrupts the dissolution of gypsum when MA worked. Despite incomplete dissolution of gypsum, the intensity of peak concerned with ettringite that is produced in MA samples shows little difference between the pastes. The intensity of portlandite from MA-free samples was higher regardless of the existence of limestone and the creation of portlandite was not sure in MA samples. This outcome agrees with the result of TG (fig. 12). This incident about CH was detected in many research about various alkanolamine additives [25] [26] [31] and Zhang et al. [32] proposed the distorted actinomorphic CH makes a negative effect on the early compressive strength. The dissolution of ferrite had hardly progressed in all samples.

The gypsum had been fully decomposed in LS0_0 until 1 day due to a relatively high ratio of clinker and gypsum. In contrast, the gypsum of LS10_0 and LS20_0 remained as the content of clinker

was decreased by substituting limestone. In the case of LS10_0, compared with LS20_0, the considerably progressed dissolution of gypsum was observed, as this result can be seen in XRD result [33], [34]. The intensity of portlandite was slightly increased as limestone replacement was improved in the samples that MA was not applied due to the accelerating effect of calcite [5], [18]. The peak of gypsum was moderately lowered by increasing the displacement of limestone in MA samples, which means the dissolution of gypsum was enhanced by limestone when alkanolamine was utilized. The modification in the calcite peak was not discovered as the contribution of calcite to the secondary hydration had not yet occurred on the first day
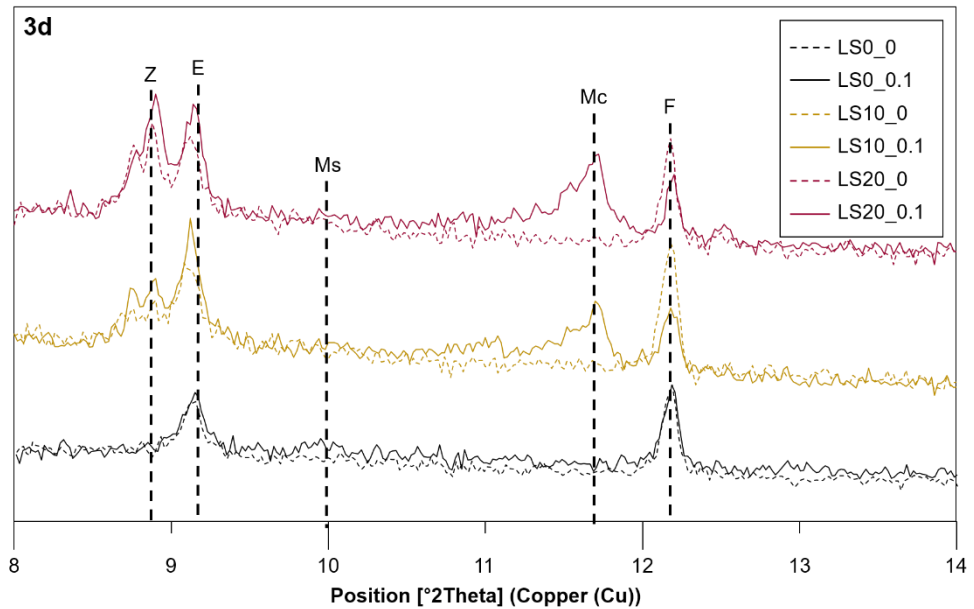
Figure 14. . XRD patterns of 3 days hydrated PLC paste samples(Z: zeolite, E: Ettringite, Mc: Monocarboaluminate, F: Ferrite).

Fig. 14 illustrates the XRD patterns of pastes that were hydrated till 3 days. In this figure, AFm phases (Mc and Ms) was observed in the activated samples as the secondary hydration occurred by enhancing the reactivity of ferrite due to an alkanolamine agent. the peak of Mc was conspicuous, on the other hand, Ms just showed the hump around 10° owing to its low crystallinity and overdue formation at room temperature [20, 35]. The peak of ferrite represents that the reactivity was advanced by MA. Accordingly, ettringite was also produced more due to the high content of aluminum from ferrite. On the contrary, the formation of AFm phases was not founded in all samples without MA and ettringite was also formed less due to lack

of aluminum ion. The generation of AFm and AFt phases caused the compressive strength of pastes to be improved on 3 days

The reactivity of ferrite was not much distinguishable between LS0_0 and LS0_0.1 on 3 days since the anion to react with aluminum from ferrite was only SO_4^{2-}. When the limestone was present in the cement matrix, the decomposition of ettringite was not shown, rather, Mc produced from calcite had ettringite stabilized [5, 18]. Limestone had no achievement on the improvement of ferrite reaction in the cement without alkanolamine and the ferrite reactivity enhancement effect of alkanolamine is more beneficial to PLC. Albeit the limestone replacement was increased more than 10 %, the quantity of Mc was not much different as seen in LS10_0.1 and LS20_0.1 on 3 days owing to the declined amount of clinker.

Figure 15. XRD patterns of 7 days hydrated PLC paste samples (Z: zeolite, E: Ettrinigte, Hc: hemicarboaluminte, Mc: Monocarboaluminate, F: Ferrite).

The above-described hydration reaction trend continued on 7 days hydrated samples (fig. 15). The formation of Ms was more progressed, as can be checked in LS0_0.1, in which the peak of Ms, not a hump, was detected and this progress made the ettringite decomposed. Hc, the OH− in the interlayer is partially substituted with CO32−, was also noticed in LS10_0.1 and LS20_0.1. The ferrite in mechanochemically activated PLC was almost dissolved and generated AFm phases (Mc and Hc), and these carbonated AFm phases did not induce the disassembly of ettringite. The difference

of ferrite reactivity between LS0 samples appeared but not much like PLC pastes.
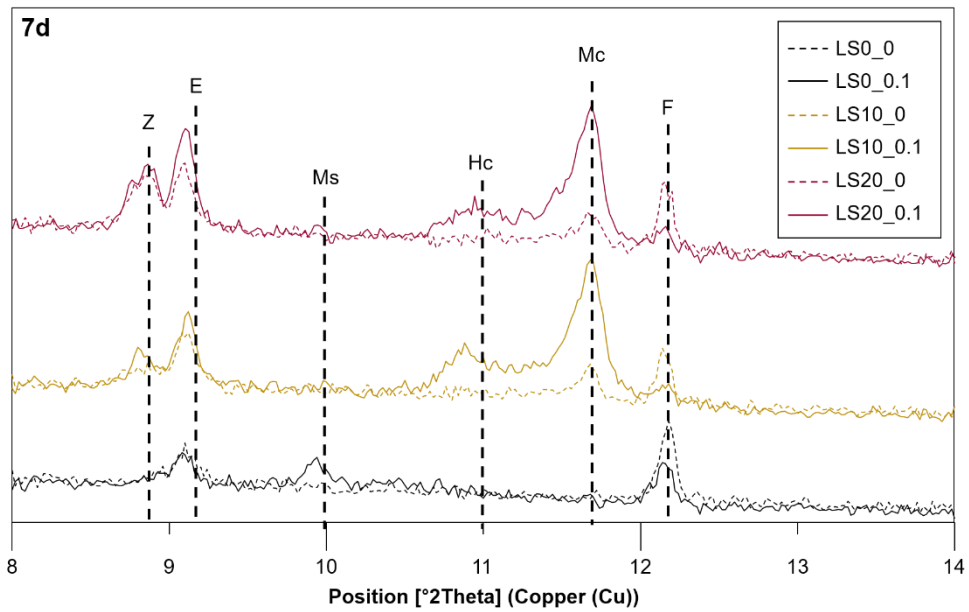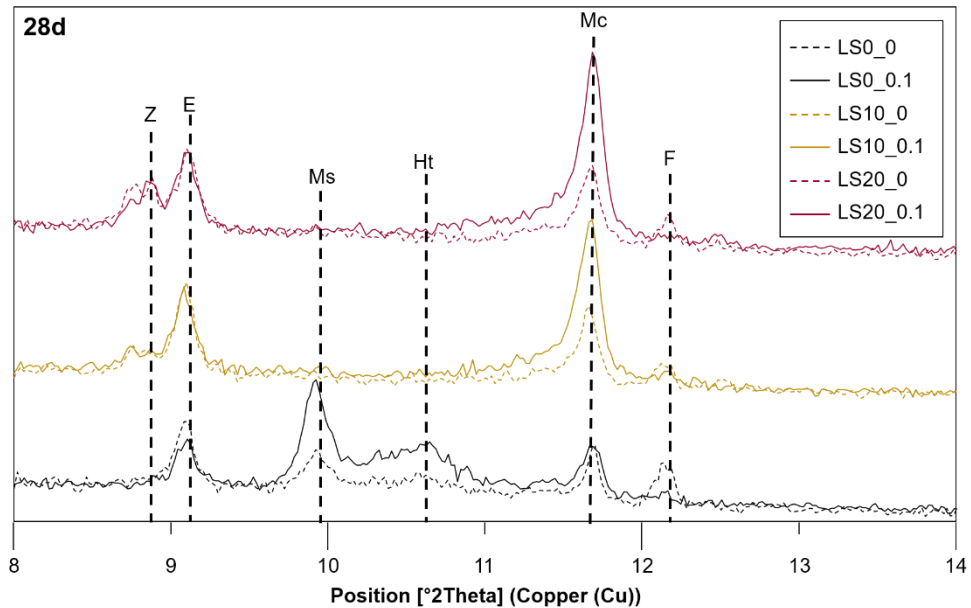

Figure 16. XRD patterns of 28 days hydrated PLC paste samples (Z : Zeolite, E: Ettrinigte, Mc : Monocarboaluminate, F : Ferrite).

XRD patterns of 28 days hydrated samples is shown in fig. 16. The Hc which appeared in 7 days vanished and became Mc as the more amount of calcite participated in the hydration reaction, which suggests that the hydration of calcite was ongoing in MA PLC after 7 days. The peak of Ms was detected in both LS0_0.1 and LS0_0, however, it was higher in the mechanochemically activated samples, which means that the decomposition of ettringite was further advanced. This breakdown of ettringite is the reason why the

3 3

compressive strength of PLC, even on the 20 % substitution of limestone, was higher than the limestone-free sample in the MA-applied sample. Although the presence of AFm phases was proved in all samples regardless of MA, the significant difference in intensity existed in accordance with mechanochemical activation. The ferrite peak nearly vanished in all MA samples, on the contrary, the peak remained in the samples which were not chemically activated.
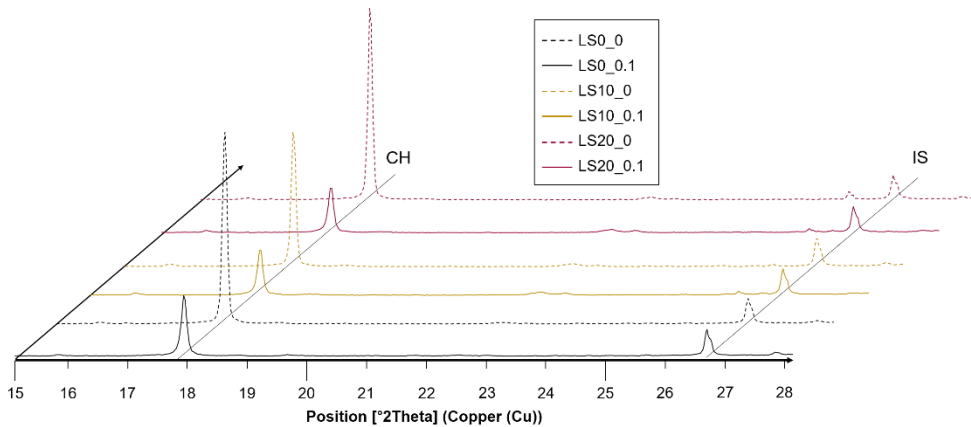
Figure 17. XRD patterns that containing the peak of portlandite on 28 days hydration (CH: portlandite, IS: internal standard material.)

The (0 0 1) peak of portlandite, which can represent the impact of alkanolamine on crystal growth, is displayed in fig. 17. The alkanolamine$-Ca^{2+}$ complex hinders the expansion of CH and postpones the precipitation of CH [25, 36]. Wang et al. [26] observed the irregular flake shaped CH which has low crystalline in the cement pastes when DEIPA and EDIPA were used as an activator. The growth of CH crystalline to (0 0 1) direction denoted as the peak of about 18 ° in XRD patterns was diminished by MA. The amount of CH was lowered by about 30 % on 28 days, however, the intensity dissimilarity was about twice in XRD patterns. When the alkanolamine was used as a grinding aid, alkanolamine not only impedes the generation of CH but also inhibits the preferred orientation of (0 0 1) direction. As a result, any relationship between CH peaks and the

amount of CH could not be revealed from MA-free samples. On the contrary, the intensity of CH peaks was decreased as the quantity of CH declined in the MA samples.
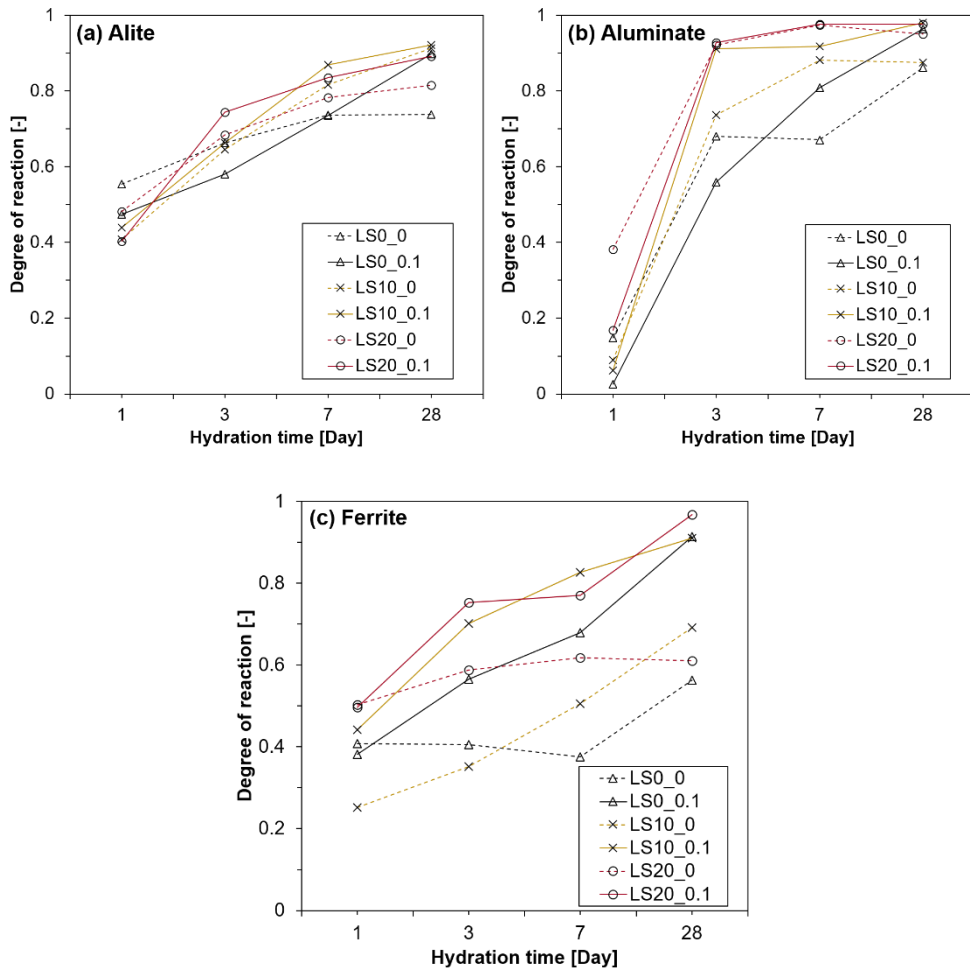

Figure 18. Evolution of the reaction degree of the clinker phases by Rietveld method.

The reaction degree of the cement clinker phases is represented in fig. 18. On the later hydration age, The C_3S in the cement with MA was more reacted than normal samples at the same replacement of limestone (fig. 18(a)). The dissolution of C_3S in LS20 and LS10 pastes was postponed by MA on the first day of hydration and the case of LS20_0.1 was more severe due to the synergic retardation effect of the large ratio of gypsum and clinker and alkanolamine. On the other hand, C_3S demonstrated the developed reactivity in LS10 sample when MA was applied, which can be elucidated by the accelerating influence of limestone and specific surface area [5, 18]. In the limestone−free samples, as the degree of C_3S hydration of LS0_0.1 sample could not catch up with LS0_0 sample until 7 days, the delay effect of alkanolamine was more fatal than PLC pastes. The C_3S in PLC was more reactive till 3 days as the substitution of limestone was increased from 10 % to 20 %.

The reactivity of C_3A was declined by MA on the first day, as can be seen in fig. 18(b). All the pastes with MA showed better dissolution of C_3A on the 28 days, which matches with other research[26, 37]. The reaction of aluminate in LS0 samples revealed that the aluminate was less responsive when MA was used. Then, the improvement of C_3A reactivity was observed after 7 days. On the other hand, the existence of limestone in the composite made the

reactivity of aluminate improved after 3 days even in the MA samples. Huang et al. [38] reported that the aluminate reaction in limestone-calcined clay cement was accelerated by alkanolamines during early hydration. The mechanochemically activated limestone powder has the important role for enhancing the aluminate reaction by promoting the precipitation of AFm phases (Mc and Hc).

At the exact content of limestone powder, the more amount of ferrite in all samples that were ground with MA participated in the hydration reaction after 3 days (Fig. 18(c)). The reactivity of ferrite had almost doubled at the later age of hydration when MA was used since the complexation of iron ion and activator makes the enhanced dissolution of ferrite [25, 26, 39]. The ferrite with MA in the presence of limestone was more reactive after 3 days, which resulted in the amelioration of AFm phases production in the cement matrix. Despite the improved dissolution of ferrite and the enrichment of iron ions in pore solution, Fe-containing AFm phases (Fe-monocarbonate, Fe-hemicarbonate, and Fe-monosulfate) did not exist and Fe-siliceous hydrogarnet was present [30, 40, 41].
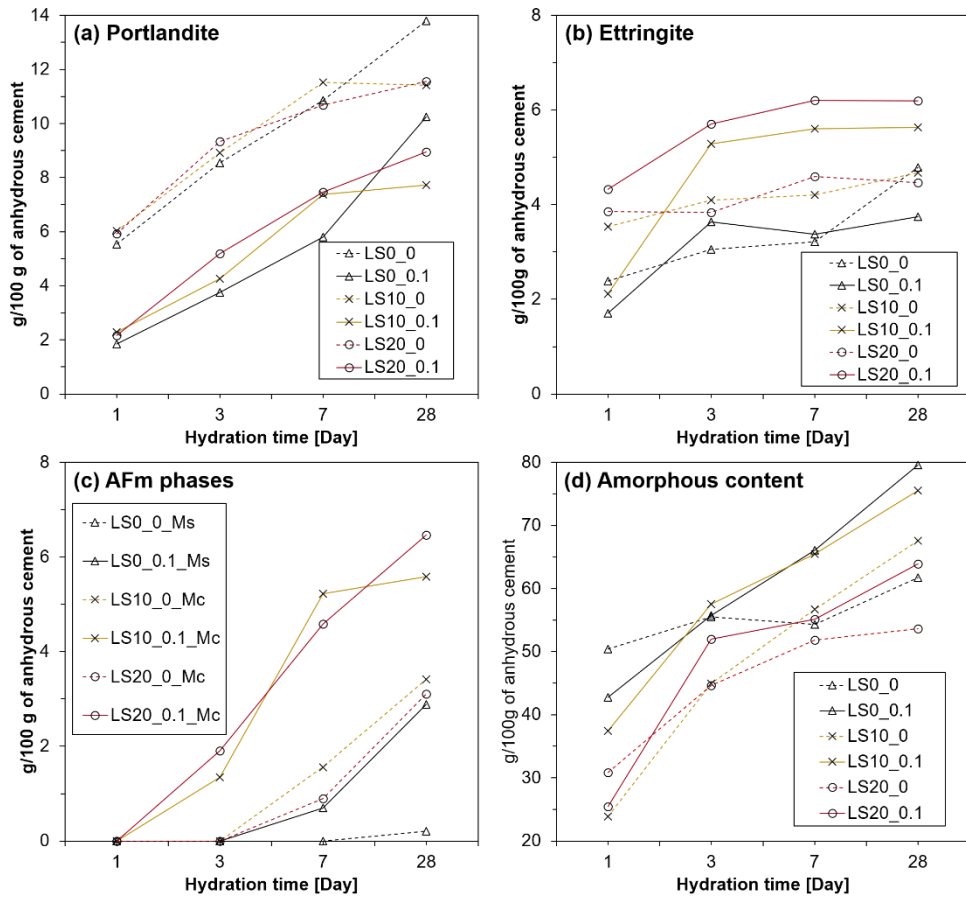
Figure 19. QXRD results of hydration products (a) portlandite, (b) ettringite, (c) AFm phases (d) amorphous content (Mc: monocarboaluminate, Ms: monosulfate).

The QXRD result of hydration products is represented in fig. 19. Portlandite in the cement pastes with MA was generated less than MA−free samples during all hydration time. Derived from this result, the Ca^{2+} ion which could precipitate with other ions in the pore solution became more dense hydration products such as C−S−H and Fe−siliceous hydrogarnet that could not be detected by XRD. The

more amount of amorphous content which includes C−S−H, Fe−siliceous hydrogarnet, and part of AFm and AFt phases that have too poor crystalline to be observed in the XRD pattern, on the contrary, was yielded from the internal standard method hydration when MA was used after 3 days hydration. This can also be the reason why the compressive strength of MA samples was higher.

The ettringite that was produced in PLC had a larger amount due to the decomposition of ettringite to Ms, which was caused by the absence of calcite. However, the decomposition of ettringite was not observed in LS0_0 paste on account of the lack of aluminum ion. Replacing clinker with limestone made the ratio of gypsum and clinker higher, which resulted in LS20_0.1 pastes holing ettringite more than LS10_0.1 paste. The enrichment of aluminum ion in pore solution had the more amount of AFm phases generated during hydration (Fig, 19(c)). Mc has the stabilization impact on the ettringite [5, 18], which caused the high compressive strength of PLC. The formation of all AFm phases was later and less when the MA was not used and the time to be detected for Mc was faster than Ms. The fact that ferrite was more reacted and Mc was more generated in LS20_0.1 than LS10_0.1 implies that mechanically increasing the specific surface area of limestone can achieve the enhanced participation of limestone with the synergetic effect of chemical activation

4. Conclusion

In the cement-concrete industry based on decarbonization of limestone, carbon neutrality is a difficult goal to achieve in reality. However, many efforts are currently being made in the United States and Europe to reduce carbon dioxide generated by the cement industry, and as part of that effort, limestone mixed cement containing up to 35% of limestone has been commercialized.

In this study, thermodynamic modeling and experiments were conducted to develop limestone mixed cement that has not yet been developed in Korea. To this end, the chemical changes that occur when the limestone content is increased based on the mineralogical composition of type 1 OPC currently used in Korea were examined. In addition, based on these results, a plan was proposed to compensate for the possible performance reduction in the development of Korean limestone cement by increasing the limestone content.

In this study, the following conclusions can be obtained.

- In the type1 OPC currently used in Korea, limestone does not actively participate in hydration reactions, so it is confirmed that an increase in limestone content in this environment reduces the mechanical performance of cement paste.

4 1

- Though the water-binder ratio (W/B) is raised, limestone still did not participate in the hydration reaction, rather, the reduction in mechanical performance due to the increase in porosity may be larger than that of ordinary Portland cement.

- In order to improve the mechanical performance of cement containing a large amount of limestone, it is necessary to change the composition of cement. In particular, in order to participate in the hydration reaction of limestone, the content of C_3A in the clinker must be increased. C_3A and limestone participate together in hydration reactions to form Mc, which contributes to improved mechanical performance and durability due to reduced voids.

- The compressive strength of all mechanochemically activated samples was weakened on the first day owing to delayed hydration reaction. However, it overtook the MA-free sample from 3 days and the LS10_0.1 had the strongest compressive strength on 28 days.

- It can be concluded that the even just usage of 0.1 % activator becomes the key to the reduction of CO_2 emission by improving the compressive strength of PLC owing to the developed specific surface area of limestone, the reactivity of ferrite, the production of AFm phases, the stabilization of

ettringite, and the generation of dense hydration product which is caused by lowered portlandite production.

In this study, the hydration reaction of cement containing high limestone was predicted based on thermodynamic modeling, and the problems caused by this were presented. Furthermore, solutions to these problems were also presented based on thermodynamic modeling as an experimental method. Therefore, it is believed that the analysis of the hydration reaction of limestone cement can contribute to the carbon neutrality of the cement－concrete industry by advancing the development and commercialization of Korean limestone cement.

Bibliography

1. Gartner, E., *Industrially interesting approaches to "low-CO2" cements.* Cement and Concrete Research, 2004. **34**(9): p. 1489-1498.

2. Lothenbach, B., K. Scrivener, and R.D. Hooton, *Supplementary cementitious materials.* Cement and Concrete Research, 2011. **41**(12): p. 1244-1256.

3. Juenger, M.C.G., R. Snellings, and S.A. Bernal, *Supplementary cementitious materials: New sources, characterization, and performance insights.* Cement and Concrete Research, 2019. **122**: p. 257-273.

4. Hawkins, P., P.D. Tennis, and R.J. Detwiler, *The use of limestone in Portland cement: a state-of-the-art review.* 1996: Portland Cement Association Skokie, IL, USA.

5. Lothenbach, B., et al., *Influence of limestone on the hydration of Portland cements.* Cement and Concrete Research, 2008. **38**(6): p. 848-860.

6. Ramezanianpour, A.A., et al., *Influence of various amounts of limestone powder on performance of Portland limestone cement concretes.* Cement and Concrete Composites, 2009. **31**(10): p. 715-720.

7. Ramezanianpour, A.M. and R.D. Hooton, *A study on hydration, compressive strength, and porosity of Portland-limestone cement mixes containing SCMs.* Cement and Concrete Composites, 2014. **51**: p. 1-13.

8. Allmann, R. and R. Hinek, *The introduction of structure types into the Inorganic Crystal Structure Database ICSD.* Acta Crystallographica Section A: Foundations of Crystallography, 2007. **63**(5): p. 412-417.

9. Gražulis, S., et al., *Crystallography Open Database (COD): an open-access collection of crystal structures and platform for world-wide collaboration.* Nucleic acids research, 2012. **40**(D1): p. D420-D427.

10. Wagner, T., et al., *GEM-Selektor geochemical modeling package: TSolMod library and data interface for multicomponent phase models.* The Canadian Mineralogist, 2012. **50**(5): p. 1173-1195.

11. Kulik, D.A., et al., *GEM-Selektor geochemical modeling package: revised algorithm and GEMS3K numerical kernel for coupled simulation codes.* Computational Geosciences, 2013. **17**(1): p. 1-24.

12. Lothenbach, B., et al., *Cemdata18: A chemical thermodynamic database for hydrated Portland cements and alkali-activated materials.* Cement and Concrete Research, 2019. **115**: p. 472-506.

13. HELGESON, H., *THEORETICAL PREDICTION OF THE THERMODYNAMIC BEHAVIOR OF AQUEOUS ELECTROLYTES BY HIGH PRESSURES AND TEMPERATURES; IV, CALCULATION OF ACTIVITY COEFFICIENTS, OSMOTIC COEFFICIENTS, AND APPARENT MOLAL AND STANDARD AND RELATIVE PARTIAL MOLAL PROPERTIES TO 600OC AND 5KB.* 1981.

14.   Lothenbach, B., et al., *Thermodynamic modelling of the effect of temperature on the hydration and porosity of Portland cement.* Cement and Concrete Research, 2008. **38**(1): p. 1-18.

15.   Zhang, J. and G.W. Scherer, *Comparison of methods for arresting hydration of cement.* Cement and Concrete Research, 2011. **41**(10): p. 1024-1036.

16.   Kang, H. and J. Moon, *Secondary curing effect on the hydration of ultra-high performance concrete.* Construction and Building Materials, 2021. **298**.

17.   Snellings, R., et al., *Report of TC 238-SCM: hydration stoppage methods for phase assemblage studies of blended cements—results of a round robin test.* Materials and structures, 2018. **51**(4): p. 1-12.

18.   Matschei, T., B. Lothenbach, and F.P. Glasser, *The role of calcium carbonate in cement hydration.* Cement and Concrete Research, 2007. **37**(4): p. 551-558.

19.   Lian, C., Y. Zhuge, and S. Beecham, *The relationship between porosity and strength for porous concrete.* Construction and Building Materials, 2011. **25**(11): p. 4294-4298.

20.   Matschei, T., B. Lothenbach, and F. Glasser, *The AFm phase in Portland cement.* Cement and concrete research, 2007. **37**(2): p. 118-130.

21.   Idiart, A.E., C.M. López, and I. Carol, *Chemo-mechanical analysis of concrete cracking and degradation due to external sulfate attack: A meso-scale model.* Cement and Concrete Composites, 2011. **33**(3): p. 411-423.

22.   Lothenbach, B., et al., *Effect of temperature on the pore solution, microstructure and hydration products of Portland cement pastes.* Cement and Concrete Research, 2007. **37**(4): p. 483-491.

23.   Taylor, H.F., *Cement chemistry*. Vol. 2. 1997: Thomas Telford London.

24.   Quennoz, A. and K.L. Scrivener, *Hydration of C3A–gypsum systems.* Cement and concrete research, 2012. **42**(7): p. 1032-1041.

25.   Ma, S., et al., *Study on the hydration and microstructure of Portland cement containing diethanol-isopropanolamine.* Cement and Concrete Research, 2015. **67**: p. 122-130.

26.   Wang, Y., et al., *Effect of diethanolisopropanolamine and ethyldiisopropylamine on hydration and strength development of Portland cement.* Cement and Concrete Research, 2022. **162**.

27.   Péra, J., S. Husson, and B. Guilhot, *Influence of finely ground limestone on cement hydration.* Cement and Concrete Composites, 1999. **21**(2): p. 99-105.

28.   Hargis, C.W., A. Telesca, and P.J. Monteiro, *Calcium sulfoaluminate (Ye'elimite) hydration in the presence of gypsum, calcite, and vaterite.* Cement and Concrete Research, 2014. **65**: p. 15-20.

29.   Ramachandran, V.S., *Influence of triethanolamine on the hydration characteristics of tricalcium silicate.* Journal of Applied Chemistry and Biotechnology, 1972. **22**(11): p. 1125-1138.

30. Dilnesa, B.Z., et al., *Fe-containing phases in hydrated cements.* Cement and Concrete Research, 2014. **58**: p. 45-55.

31. Zhang, Y., et al., *A further understanding on the strength development of cement pastes in the presence of triisopropanolamine used in CRTS III slab track.* Construction and Building Materials, 2022. **315**: p. 125743.

32. Zhang, Y., et al., *Influences of triethanolamine on the performance of cement pastes used in slab track.* Construction and Building Materials, 2020. **238**: p. 117670.

33. Singh, M., *Influence of blended gypsum on the properties of Portland cement and Portland slag cement.* Cement and concrete research, 2000. **30**(8): p. 1185-1188.

34. Bhanumathidas, N. and N. Kalidas, *Dual role of gypsum: Set retarder and strength accelerator.* The Indian Concrete Journal, 2004. **78**: p. 1-4.

35. Damidot, D. and F. Glasser, *Thermodynamic investigation of the CaO Al2O3 CaSO4 H2O system at 50° C and 85° C.* Cement and Concrete Research, 1992. **22**(6): p. 1179-1191.

36. Wang, J., et al., *Effect of chelating solubilization via different alkanolamines on the dissolution properties of steel slag.* Journal of Cleaner Production, 2022. **365**: p. 132824.

37. Li, W., et al., *The mechanochemical process and properties of Portland cement with the addition of new alkanolamines.* Powder Technology, 2015. **286**: p. 750-756.

38. Huang, H., et al., *Strength-promoting mechanism of alkanolamines on limestone-calcined clay cement and the role of sulfate.* Cement and Concrete Research, 2021. **147**: p. 106527.

39. Lu, Z., et al., *A comparative study of the effects of two alkanolamines on cement hydration.* Advances in Cement Research, 2022. **34**(2): p. 47-56.

40. Dilnesa, B.Z., et al., *Iron in carbonate containing AFm phases.* Cement and Concrete Research, 2011. **41**(3): p. 311-323.

41. Dilnesa, B.Z., et al., *Synthesis and characterization of hydrogarnet Ca3(AlxFe1−x)2(SiO4)y(OH)4(3−y).* Cement and Concrete Research, 2014. **59**: p. 96-111.

Abstract

스마트 구조 결합재 개발을 위한 실험적 및 열역학적 연구

전세계적으로 사회기반시설 구축에 사용되고 있는 보통 포틀랜드 시멘트의 경우 이산화탄소 다배출재료로서 현재 국제적으로 이슈화되고 있는 탄소중립이라는 목표를 달성하기 위해서는 보다 친환경적이고 스마트한 재료의 개발이 필요하다. 미국과 유럽에서는 시멘트계 재료의 친환경성을 높이고자 하는 노력을 오랫동안 진행하여 왔으며, 이미 35 %의 석회석을 혼합한 스마트 구조 결합재의 상용화가 완료되었다. 그러나 한국에서는 5%의 혼입만 허용하고 있다.

본 연구에서는 기존 재료에 석회석 혼입양을 증진시켜 친환경성을 확보하는 것을 목표로 하였다. 열역학적 모델링을 활용하여 1종 보통 포틀랜드 시멘트의 석회석함량을 변화시키며 발생하는 수화반응의 변화에 대해 연구하였다. 압축강도 및 수화열 측정, 열중량 분석과 같은 실험을 진행함과 동시에 X선 회절 분석과 리트벨트 정량분석을 활용하여 수화 반응을 분석하였다. 열역학적 모델링 결과 1종 보통 포틀랜드 시멘트에서 석회석의 함량이 증가하더라도 석회석은 수화반응에 참여하지 않았으며 이로 인해서 시멘트 페이스트의 역학적 성능은 감소할 것으로 예측되었다. 이러한 역학적 성능 감소는 다양한 물−시멘트비에도 동일하게 관측되었다. 시멘트에 존재하는 알루미나 광물의 함량을 증가시키면 모노카르보알루미네이트가 생성되며 석회석이 수화반응에 참여하고 역학

적 성능에 긍정적인 영향을 주었으며, 양생온도도 중요한 역할을 하는 것을 확인하였다. 실제 실험에서 알루미나 광물의 반응을 물리화학적으로 촉진시킨 경우 모노카르보알루미네이트의 생성이 향상되었으며 이로 인해서 20 %의 클링커를 석회석으로 치환하더라도 석회석 혼합 시멘트의 압축강도가 증가하였다. 현재 한국에서 석회석 혼합시멘트를 개발할 경우 높은 분말도, 알루미나 함량 및 적절한 양생온도가 역학적 성능감소를 막아줄 수 있는 공학적인 방법으로 제안되었다.